

Carrier and Clock recovery in (turbo) coded systems: Cramer-Rao Bound and Synchronizer Performance

N. Noels, H. Steendam and M. Moeneclaey

TELIN department, Ghent University, St-Pietersnieuwstraat 41, B-9000 GENT,
BELGIUM

Tel: (+32) 9 264 34 26, Fax: (+32) 9 264 42 95

Mailto: {nnoels, hs, mm} @telin.UGent.be

ABSTRACT

In this paper we derive the Cramer-Rao bound (CRB) for joint carrier phase, carrier frequency and timing estimation from a noisy linearly modulated signal with *encoded* data symbols. We obtain a closed-form expression for the CRB in terms of the marginal a posteriori probabilities of the coded symbols, allowing efficient numerical evaluation of the CRB for a wide range of coded systems by means of the BCJR algorithm [1].

Simulation results are presented for a rate $\frac{1}{2}$ turbo code combined with QPSK mapping. We point out that the synchronization parameters for the coded system are essentially decoupled. We find that, at the normal (i.e., low) operating SNR of the turbo-coded system, the *true* CRB for *coded* transmission is (i) essentially the same as the *modified* CRB from [2,3], and (ii) considerably smaller than the *true* CRB for *uncoded* transmission from [4-7]. Comparison of actual synchronizer performance with the CRB for turbo-coded QPSK reveals that the 'code-aware' soft Decision Directed *turbo synchronizer* presented in [8] performs very closely to this CRB, whereas 'code-unaware' estimators such as the conventional *Non Data Aided* algorithm are substantially worse; when operating on coded signals, the performance of the latter synchronizers is still limited by the CRB for uncoded transmission.

Keywords: carrier recovery, clock recovery, coded systems, Cramer-Rao bound, synchronizer performance

I. INTRODUCTION

The impressive performance of turbo receivers implicitly assumes perfect synchronization, i.e., the carrier phase, frequency offset and time delay must be recovered accurately before data detection. Synchronization for turbo-encoded systems is yet a very challenging task since the receiver usually operates at extremely low SNR values. The development of accurate synchronization techniques has therefore recently received a lot of attention in the technical literature.

A common approach to judge the performance of parameter estimators is to compare their resulting mean-square error (MSE) with the Cramer-Rao bound (CRB), which is a fundamental lower bound on the error variance of unbiased estimators [9]. In order to avoid the computational complexity related to the *true* CRB, a *modified* CRB (MCRB) has been derived in [2,3]. The MCRB is much simpler to evaluate than the CRB, but is in general looser (i.e., lower) than the CRB, especially at low SNR. In [4-7], the CRB for the estimation of carrier phase, carrier frequency and timing delay from *uncoded* data symbols has been obtained and discussed. In [10], the CRB for carrier phase estimation from *coded* data has been expressed in terms of the marginal a posteriori probabilities (APPs) of the coded symbols.

In this contribution we derive the CRB for *joint* carrier phase, carrier frequency offset and timing recovery in *coded* systems. Again we obtain a closed-form expression for the CRB in terms of the marginal APPs, allowing the numerical evaluation of the bound for a wide range of coded systems, including schemes with iterative detection (turbo schemes). This CRB is evaluated for rate $\frac{1}{2}$ turbo-coded QPSK, and compared to (i) the MCRB, (ii) the CRB for uncoded transmission, and (iii) the MSE of some practical synchronizers. Our results point out that, at the normal operating SNR of the turbo code, (i) the CRB is essentially the same as the MCRB, (ii) the CRB is significantly smaller than the CRB for uncoded transmission, and (iii) the CRB is a tight lower bound on the MSE resulting from the joint synchronization and turbo decoding scheme the authors proposed in [8].

II. PROBLEM FORMULATION

Consider an observation vector \mathbf{r} with a probability density function $p(\mathbf{r};\mathbf{u})$ that depends on a deterministic vector parameter \mathbf{u} . Suppose that from the observation \mathbf{r} , one is able to produce an *unbiased* estimate $\hat{\mathbf{u}}$ of the parameter \mathbf{u} , i.e., $E_{\mathbf{r}}[\hat{\mathbf{u}}] = \mathbf{u}$ for all \mathbf{u} ; the expectation $E_{\mathbf{r}}[\cdot]$ is with respect to $p(\mathbf{r};\mathbf{u})$. Then the estimation error variance is lower bounded by the CRB [9]: $E_{\mathbf{r}}[(\hat{u}_i - u_i)^2] \geq CRB_i(\mathbf{u})$, where $CRB_i(\mathbf{u})$ is the i -th diagonal element of the inverse of the *Fisher information matrix* (FIM) $\mathbf{J}(\mathbf{u})$. The (i,j) -th element of $\mathbf{J}(\mathbf{u})$ is given by

$$\mathbf{J}_{i,j}(\mathbf{u}) = E_{\mathbf{r}} \left[-\frac{\partial^2}{\partial u_i \partial u_j} \ln(p(\mathbf{r};\mathbf{u})) \right] = E_{\mathbf{r}} \left[\frac{\partial}{\partial u_i} \ln(p(\mathbf{r};\mathbf{u})) \frac{\partial}{\partial u_j} \ln(p(\mathbf{r};\mathbf{u})) \right]. \quad (1)$$

The probability density $p(\mathbf{r};\mathbf{u})$ of \mathbf{r} , corresponding to a given value of \mathbf{u} , is called the *likelihood function* of \mathbf{u} , while $\ln(p(\mathbf{r};\mathbf{u}))$ is the *log-likelihood function* of \mathbf{u} . Note that $\mathbf{J}(\mathbf{u})$ is a symmetrical matrix. When the element $\mathbf{J}_{i,j}(\mathbf{u}) = 0$, the parameters u_i and u_j are said to be *decoupled*.

When the observation \mathbf{r} depends not only on the parameter \mathbf{u} to be estimated but also on a nuisance vector parameter \mathbf{v} , the likelihood function of \mathbf{u} is obtained by averaging the likelihood function $p(\mathbf{r}|\mathbf{v};\mathbf{u})$ of the vector (\mathbf{u},\mathbf{v}) over the a priori distribution of the nuisance parameter: $p(\mathbf{r};\mathbf{u}) = E_{\mathbf{v}}[p(\mathbf{r}|\mathbf{v};\mathbf{u})]$. We refer to $p(\mathbf{r}|\mathbf{v};\mathbf{u})$ as the *joint* likelihood function, as $p(\mathbf{r}|\mathbf{v};\mathbf{u})$ is relevant to the joint estimation of \mathbf{u} and \mathbf{v} .

Let us consider the complex baseband representation $r(t)$ of a noisy linearly modulated signal :

$$r(t) = \sum_{k=-K}^K a_k h(t - kT - \tau) \exp(j(\theta + 2\pi F t)) + w(t), \quad (2)$$

where $\mathbf{a} = (a_{-K}, \dots, a_K)$ is a vector of $L = 2K+1$ symbols taken from an M-PSK, M-QAM or M-PAM constellation according to a combination of an encoding rule and a mapping rule; $h(t)$ is an even, *real-valued* unit-energy square-root Nyquist pulse; τ is the time delay; θ is the carrier phase at $t = 0$; F is the carrier frequency offset; T is the symbol interval; $w(t)$ is complex-valued zero-mean Gaussian noise with independent real and imaginary parts, each having a normalized power spectral density of $N_0/(2E_s)$, with E_s and N_0 denoting the symbol energy and the noise power spectral density, respectively.

With $\mathbf{u} = (u_1, u_2, u_3) = (\theta, F, \tau)$ and $\mathbf{v} = \mathbf{a}$, the joint likelihood function $p(\mathbf{r}|\mathbf{v};\mathbf{u})$ resulting from (2) is Gaussian, with a mean depending on (\mathbf{u},\mathbf{v}) and a covariance matrix that is independent of (\mathbf{u},\mathbf{v}) . Within a factor not depending on (\mathbf{u},\mathbf{v}) , $p(\mathbf{r}|\mathbf{v};\mathbf{u})$ is given by

$$p(\mathbf{r}|\mathbf{v};\mathbf{u}) = p(\mathbf{r}|\mathbf{a};\theta, F, \tau) = \prod_{k=-K}^K F(a_k, \tilde{z}_k(\theta, F, \tau)), \quad (3)$$

where

$$F(a_k, \tilde{z}_k(\theta, F, \tau)) = \exp\left(\frac{E_s}{N_0} \left(2 \operatorname{Re}[a_k^* \tilde{z}_k(\theta, F, \tau)] - |a_k|^2\right)\right). \quad (4)$$

In (3), \mathbf{r} is a vector representation of the signal $r(t)$ from (2), and $\tilde{z}_k(\theta, F, \tau) = z_k(F, \tau)e^{-j\theta}$, where $z_k(F, \tau)$ is defined as

$$z_k(F, \tau) = \int e^{-j2\pi F t} r(t) h(t - kT - \tau) dt. \quad (5)$$

Note that $\tilde{z}_k(\theta, F, \tau)$ is obtained by first frequency-correcting $r(t)$ by an amount $-F$, then applying the result to a filter that is matched to the transmit pulse $h(t)$ and sampling the matched filter output at instant $kT+\tau$, and finally rotating the resulting sample over an angle $-\theta$. Hence, \tilde{z}_k is a function of (θ, F, τ) , whereas z_k depends only on (F, τ) . The log-likelihood function $\ln(p(\mathbf{r};\mathbf{u}))$ resulting from (3) is given by

$$\ln p(\mathbf{r};\mathbf{u}) = \ln p(\mathbf{r};\theta, F, \tau) = \ln \left(E_{\mathbf{a}} \left[\prod_{k=-K}^K F(a_k, \tilde{z}_k(\theta, F, \tau)) \right] \right). \quad (6)$$

The expectation $E_{\mathbf{a}}[\cdot]$ in (6) is with respect to the a priori distribution $p(\mathbf{a})$ of the transmitted data sequence \mathbf{a} . Computation of the CRB requires the substitution of (6) into (1), and the evaluation of the various expectations included in (6) and (1).

The evaluation of the expectations involved in $\mathbf{J}(\theta, F, \tau)$ and $p(\mathbf{r}; \theta, F, \tau)$ is quite tedious. In order to avoid the computational complexity caused by the nuisance parameters, a simpler lower bound, called the modified CRB (MCRB), has been derived in [2,3], i.e., $E_{\mathbf{r}}[(\hat{u}_i - u_i)^2] \geq \text{CRB}_i(\mathbf{u}) \geq \text{MCRB}_i(\mathbf{u})$, where $\text{MCRB}_i(\mathbf{u})$ is the i -th diagonal element of the inverse of the *modified* Fisher information matrix (MFIM) $\mathbf{J}^M(\mathbf{u})$. The (i,j) -th element of $\mathbf{J}^M(\mathbf{u})$ is given by

$$\begin{aligned} \mathbf{J}_{i,j}^M(\mathbf{u}) &= E_{\mathbf{r},\mathbf{v}} \left[-\frac{\partial^2}{\partial u_i \partial u_j} \ln(p(\mathbf{r} | \mathbf{v}; \mathbf{u})) \right] \\ &= E_{\mathbf{r},\mathbf{v}} \left[\frac{\partial}{\partial u_i} \ln(p(\mathbf{r} | \mathbf{v}; \mathbf{u})) \frac{\partial}{\partial u_j} \ln(p(\mathbf{r} | \mathbf{v}; \mathbf{u})) \right] \end{aligned} \quad (7)$$

and $E_{\mathbf{r},\mathbf{v}}[\cdot]$ denotes averaging over both \mathbf{r} and \mathbf{v} , i.e., with respect to $p(\mathbf{r}, \mathbf{v}; \mathbf{u}) = p(\mathbf{r} | \mathbf{v}; \mathbf{u})p(\mathbf{v})$. When $p(\mathbf{r} | \mathbf{v}; \mathbf{u})$ is Gaussian, (7) is much simpler than (1) as far as analytical evaluation is concerned, because the tedious computation of $p(\mathbf{r}; \mathbf{u})$ is avoided.

The MCRB for joint carrier phase, carrier frequency offset and timing estimation, corresponding to $\mathbf{r}(t)$ from (1), is given by [2,3]

$$E[(\hat{\theta} - \theta)^2] \geq \text{MCRB}_\theta = \frac{N_0}{2E_s L}, \quad (8)$$

$$E[(\hat{F} - F)^2 \cdot T^2] \geq \text{MCRB}_F = \frac{3N_0}{2\pi^2 E_s L(L^2 - 1)}, \quad (9)$$

$$E[(\hat{t} - t)^2 / T^2] \geq \text{MCRB}_t = \frac{N_0}{2E_s L T^2 \int (\dot{h}(t))^2 dt}, \quad (10)$$

where $\dot{h}(t) = dh(t)/dt$ and $L = 2K+1$ denotes the number of symbols transmitted within the observation interval. Note that in (9) and (10) the frequency and timing error have been normalized by the symbol interval T . The MCRB does not depend on the symbol constellation; the shape of the transmit pulse $h(t)$ affects only the quantity $\int (\dot{h}(t))^2 dt$ in (10), which is an increasing function of the excess bandwidth of the transmit pulse $h(t)$. The MCRB for phase and timing estimation are inversely proportional to L ; the MCRB for frequency estimation is, for large L , inversely proportional to L^3 . In [11], the high-SNR limit of the true CRB related to the estimation of a scalar parameter has been evaluated analytically and has been shown to coincide with the MCRB from (8)-(10).

In the next section we derive a closed-form expression of the CRB resulting from (1) in terms of the marginal APPs of the coded symbols, allowing efficient numerical evaluation of the CRB.

III. DERIVATION OF THE CRB

The log-likelihood function $\ln(p(\mathbf{r};\theta,F,\tau))$ from (6) can be written as

$$\ln p(\mathbf{r}; \theta, F, \tau) = \ln \left(\sum_{i=0}^{M^L-1} \Pr[\mathbf{a} = \mathbf{c}_i] p(\mathbf{r} | \mathbf{c}_i; \theta, F, \tau) \right), \quad (11)$$

where $p(\mathbf{r}|\mathbf{c}_i;\theta,F,\tau)$ is given by (3) and i enumerates all M^L symbol sequences \mathbf{c}_i of length L . Denoting by ξ the set of legitimate coded sequences of length L , we have $\Pr[\mathbf{a} = \mathbf{c}_i] = M^{\rho L}$ for $\mathbf{c}_i \in \xi$ and $\Pr[\mathbf{a} = \mathbf{c}_i] = 0$ otherwise, with ρ and M denoting the rate of the code and the number of constellation points, respectively. Differentiation of (11) yields

$$\frac{\partial}{\partial \mathbf{u}_\ell} \ln(p(\mathbf{r}; \mathbf{u})) = \sum_{i=0}^{M^L-1} \frac{\Pr[\mathbf{a} = \mathbf{c}_i] p(\mathbf{r} | \mathbf{c}_i; \theta, F, \tau)}{p(\mathbf{r}; \theta, F, \tau)} \frac{\partial}{\partial \mathbf{u}_\ell} \ln(p(\mathbf{r} | \mathbf{c}_i; \mathbf{u})). \quad (12)$$

Making use of Bayes' rule, we obtain

$$\frac{\Pr[\mathbf{a} = \mathbf{c}_i] p(\mathbf{r} | \mathbf{c}_i; \theta, F, \tau)}{p(\mathbf{r}; \theta, F, \tau)} = \Pr[\mathbf{a} = \mathbf{c}_i | \mathbf{r}; \theta, F, \tau], \quad (13)$$

where $\Pr[\mathbf{a} = \mathbf{c}_i | \mathbf{r}; \theta, F, \tau]$ ($i = 0, \dots, M^L-1$) are the *joint* symbol a posteriori probabilities (APPs); note from (3) that $\Pr[\mathbf{a} = \mathbf{c}_i | \mathbf{r}; \theta, F, \tau]$ is a function of \mathbf{c}_i and $\tilde{\mathbf{z}} = (\tilde{z}_{-K}, \dots, \tilde{z}_K)^T$ only. Using (13) and (3), (12) is transformed into

$$\frac{\partial}{\partial \mathbf{u}_\ell} \ln(p(\mathbf{r}; \mathbf{u})) = 2 \frac{E_s}{N_0} \sum_{k=-K}^K \text{Re}(\mathbf{m}_k^*(\tilde{\mathbf{z}}) \tilde{z}_{\ell,k}), \quad (14)$$

where the subscript ℓ denotes differentiation with respect to \mathbf{u}_ℓ , i.e.,

$$\tilde{z}_{\ell,k} = \frac{\partial}{\partial \mathbf{u}_\ell} (\tilde{z}_k) \quad (15)$$

and $\mu_k(\tilde{\mathbf{z}})$ is the a posteriori average of the symbol a_k :

$$\begin{aligned} \mu_k(\tilde{\mathbf{z}}) &= \sum_{i=0}^{M^L-1} (\mathbf{c}_i)_k \Pr[\mathbf{a} = \mathbf{c}_i | \mathbf{r}; \theta, F, \tau] \\ &= \sum_{m=0}^{M-1} \alpha_m \Pr[a_k = \alpha_m | \mathbf{r}; \theta, F, \tau] \end{aligned} \quad (16)$$

In (16), $(\mathbf{c}_i)_k$ is the k -th component of the vector \mathbf{c}_i , $(\alpha_0, \alpha_1, \dots, \alpha_{M-1})$ denotes the set of constellation points, and $\Pr[a_k = \alpha_m | \mathbf{r}; \theta, F, \tau]$ ($m = 0, \dots, M-1$) are the *marginal*

symbol APPs. We emphasize that no approximation is involved when arriving at (16). The second line of (16) simply expresses the a posteriori average of a_k in terms of the marginal APP of a_k , rather than the joint APP of (a_k, \dots, a_K) .

Substitution of (14) into (1) yields an exact expression of the FIM in terms of the a posteriori symbol averages $\mu_k(\tilde{\mathbf{z}})$, which in turn depend on the marginal symbol APPs $\Pr[a_k = \alpha_m | \mathbf{r}; \theta, F, \tau]$. One obtains:

$$\mathbf{J}_{i,j} = 4 \left(\frac{E_s}{N_0} \right)^2 \sum_{k=-K}^K \sum_{k'=-K}^K E \left[\text{Re}[\mu_k^*(\tilde{\mathbf{z}}) \tilde{z}_{i,k}] \text{Re}[\mu_{k'}^*(\tilde{\mathbf{z}}) \tilde{z}_{j,k'}] \right], \quad (17)$$

where $E[\cdot]$ denotes averaging over the quantities $\tilde{\mathbf{z}}$, $\tilde{z}_{i,k}$ and $\tilde{z}_{j,k'}$. As this averaging cannot be done analytically, we have to resort to a numerical evaluation.

A brute force evaluation of the FIM involves replacing in (17) the statistical average $E[\cdot]$ by an arithmetical average over a large number of realizations of $(\tilde{\mathbf{z}}, \tilde{z}_{i,k}, \tilde{z}_{j,k'})$, that are computer-generated according to the joint distribution of $(\tilde{\mathbf{z}}, \tilde{z}_{i,k}, \tilde{z}_{j,k'})$. However, because of the correlation between the quantities $\tilde{\mathbf{z}}$, $\tilde{z}_{i,k}$ and $\tilde{z}_{j,k'}$, a brute force numerical averaging is time consuming. In Appendix, we show how the computational complexity can be reduced by performing the averaging in (17) over $\tilde{\mathbf{z}}$, $\tilde{z}_{i,k}$ and $\tilde{z}_{j,k'}$ in two steps. In the first step we average over $\tilde{z}_{i,k}$ and $\tilde{z}_{j,k'}$, conditioned on $\tilde{\mathbf{z}}$; this conditional averaging is done *analytically*. In the second step we remove the conditioning by *numerically* averaging over $\tilde{\mathbf{z}}$; the generation of realizations of $\tilde{\mathbf{z}}$ is easy, as $\tilde{\mathbf{z}} = \mathbf{a} + \mathbf{n}$ where the complex-valued zero-mean Gaussian noise vector \mathbf{n} has statistically independent components with variance N_0/E_s , and the data symbol vector \mathbf{a} results from the encoding and mapping of a randomly generated information bit sequence.

The numerical evaluation of the FIM requires the computation of the a posteriori symbol averages $\mu_k(\tilde{\mathbf{z}})$ that correspond to the realizations of the vector $\tilde{\mathbf{z}}$. These a posteriori symbol averages are given by the second line of (16) in terms of the marginal symbol APPs $\Pr[a_k = \alpha_m | \mathbf{r}; \theta, F, \tau]$. In principle, the marginal symbol APPs can be obtained as appropriate summations of joint symbol APPs $\Pr[\mathbf{a} = \mathbf{c}_i | \mathbf{r}; \theta, F, \tau]$, which in turn can be computed from (13) and (3). However, the computational complexity of this procedure increases exponentially with the sequence length L .

For codes that are described by means of a trellis, the marginal symbol APPs can be easily computed from the trellis state APPs and state transition APPs, which in turn can be determined efficiently from $\tilde{\mathbf{z}}$ by means of the Bahl-Cocke-Jelinek-Raviv (BCJR) algorithm [1]. As its computational complexity grows only linearly with the number of states and with the sequence length L , the BCJR algorithm is the appropriate tool for marginal symbol APP computation in case of linear block codes, convolutional codes and trellis codes, provided that the number of states is manageable.

When the coded symbol sequence results from the (serial or parallel) concatenation of two encoders that are separated by an interleaver (such as turbo codes [12]), the underlying overall trellis has a number of states that grows exponentially with the interleaver size. However, when the constituent encoders themselves are described by a small trellis, the state APPs and state transition APPs

of the individual trellises can be efficiently computed by means of iterated application of the BCJR algorithm to each of the trellises, with exchange of extrinsic information between the BCJR algorithms at each iteration. When the coded bits (conditioned on \mathbf{r} and (θ, F, τ)) can be considered as independent (which is a reasonable assumption when the interleaver size is large), this iterative procedure yields the correct APPs after convergence [13]. Whereas a turbo decoder makes use of the state APPs and state transition APPs (resulting from iterated application of the BCJR algorithm) to compute the log-likelihood ratios of the information bits, we use these APPs to compute the marginal symbol APPs instead.

Once we have obtained the numerical value of the 3x3 FIM (15), the CRBs related to the joint estimation of (θ, F, τ) are obtained from matrix inversion. However, in many practical situations a subset of the parameters (θ, F, τ) is estimated, assuming the remaining parameters to be perfectly known; in this case the relevant FIM is obtained by deleting from the 3x3 FIM (15) the rows and columns that correspond to the parameters that are known. Therefore, we consider the following cases.

- The CRB for the estimation of u_i jointly with u_j and u_k is given by

$$CRB_i = \frac{\mathbf{J}_{j,j}\mathbf{J}_{k,k} - \mathbf{J}_{j,k}^2}{\mathbf{J}_{i,i}\mathbf{J}_{j,j}\mathbf{J}_{k,k} - \mathbf{J}_{i,i}\mathbf{J}_{j,k}^2 - \mathbf{J}_{j,j}\mathbf{J}_{i,k}^2 - \mathbf{J}_{k,k}\mathbf{J}_{i,j}^2 + 2\mathbf{J}_{i,j}\mathbf{J}_{j,k}\mathbf{J}_{i,k}}. \quad (18)$$

- The CRB for the estimation of u_i assuming u_j and u_k to be perfectly known is given by

$$CRB_i = \frac{1}{\mathbf{J}_{i,i}}. \quad (19)$$

- The CRB for the estimation of u_i jointly with u_j assuming u_k to be perfectly known is given by

$$CRB_i = \frac{\mathbf{J}_{j,j}}{\mathbf{J}_{i,i}\mathbf{J}_{j,j} - \mathbf{J}_{i,j}^2}. \quad (20)$$

IV. NUMERICAL RESULTS AND DISCUSSION

Simulation results are obtained for the observation of $L=1001$ QPSK turbo-encoded symbols. The transmit pulse is a square-root cosine roll-off pulse with an excess bandwidth of 20% or 100%. The turbo encoder consists of the parallel concatenation of two identical recursive systematic rate 1/2 convolutional codes with generator polynomials $(37)_8$ and $(21)_8$, through a pseudo random interleaver of length L ; the output of the turbo encoder is punctured to obtain an overall rate of 1/2, and Gray-mapped onto the QPSK constellation.

As far as this simulation set-up is concerned, our numerical results indicate that $\mathbf{J}_{ij}^2 \ll \mathbf{J}_i\mathbf{J}_j$, $\forall i, j \in \{1, 2, 3\}$ and $i \neq j$. This implies that both (18) and (20) yield $CRB_i \cong 1/\mathbf{J}_i$. Comparing this result with (19) indicates that the CRB related to the estimation of a synchronization parameter (carrier phase, carrier frequency offset or timing) is essentially independent of the considered scenario (joint estimation of all three parameters, joint estimation of two parameters with the third parameter

assumed to be known, estimation of one parameter with the other two parameters assumed to be known). This means that there is almost no coupling between the parameters θ , F and τ , so that (at least for small errors) the inaccuracy in one of the parameters does not impact the estimation of the other parameters. A similar observation regarding the elements of the FIM for uncoded transmission and the MFIM (7), resulting from $r(t)$ given by (2), have been reported in [7] and [3], respectively.

For the joint estimation of θ , F and τ , Fig. 1 shows the ratio CRB/MCRB (the left ordinate) along with the BER corresponding to perfect synchronization (the right ordinate) as a function of E_s/N_0 per coded symbol (solid lines). The ratio CRB/MCRB for uncoded transmission (UC) is also displayed (dashed lines). We make the following observations.

- The ratio CRB/MCRB related to timing estimation increases with decreasing rolloff. The same behavior has been observed in [7], but for uncoded transmission only.
- The ratios CRB/MCRB related to phase estimation and frequency estimation are essentially the same, and do not depend on the shape of the transmitted square-root Nyquist pulse $h(t)$. The same behavior has been observed in [4], but for uncoded transmission only.
- Let us denote by CRB_{uncoded} and CRB_{coded} the CRBs related to uncoded and coded transmission, respectively. We observe that $CRB_{\text{uncoded}} > CRB_{\text{coded}}$. This implies that it is potentially more accurate to estimate the synchronizer parameters from coded data than from uncoded data.
- Let us restrict our attention to coded transmission. The MSE resulting from ‘code-aware’ synchronizers (that exploit code properties during the estimation proces) is lower bounded by CRB_{coded} . However, the MSE of synchronizers that do not exploit code properties (i.e., ‘code-unaware’ synchronizers) is lower bounded by CRB_{uncoded} (even when operating on coded systems). At the normal operating SNR of the turbo code (this excludes very low SNR at which the turbo code becomes unreliable, as well as very high SNR at which uncoded transmission becomes reliable), CRB_{coded} is considerably smaller than CRB_{uncoded} . It follows that code-aware synchronizers are potentially more accurate than code-unaware synchronizers when operating on coded signals. The ratio $CRB_{\text{uncoded}}/CRB_{\text{coded}}$ provides a quantitative indication *to what extent* synchronizer performance can be improved by making clever use of the code structure.
- At high SNR, the CRB converges to the MCRB; this behavior is consistent with [11]. When E_s/N_0 decreases, a critical value $(E_s/N_0)_{\text{crit}}$ is reached, below which the CRB starts to diverge from the MCRB. Fig. 1 shows that, for coded transmission, this critical value corresponds to a BER between 10^{-2} and 10^{-3} (a similar observation has been reported for uncoded transmission [7,10]: $(E_s/N_0)_{\text{crit}}$ for uncoded transmission also corresponds to $BER \cong 10^{-3}$, but exceeds $(E_s/N_0)_{\text{crit}}$ for coded transmission by an amount equal to the coding gain). This indicates that, even at the (very low) operating SNR of the coded system, the CRB is very well approximated by the MCRB (which is much simpler to evaluate).

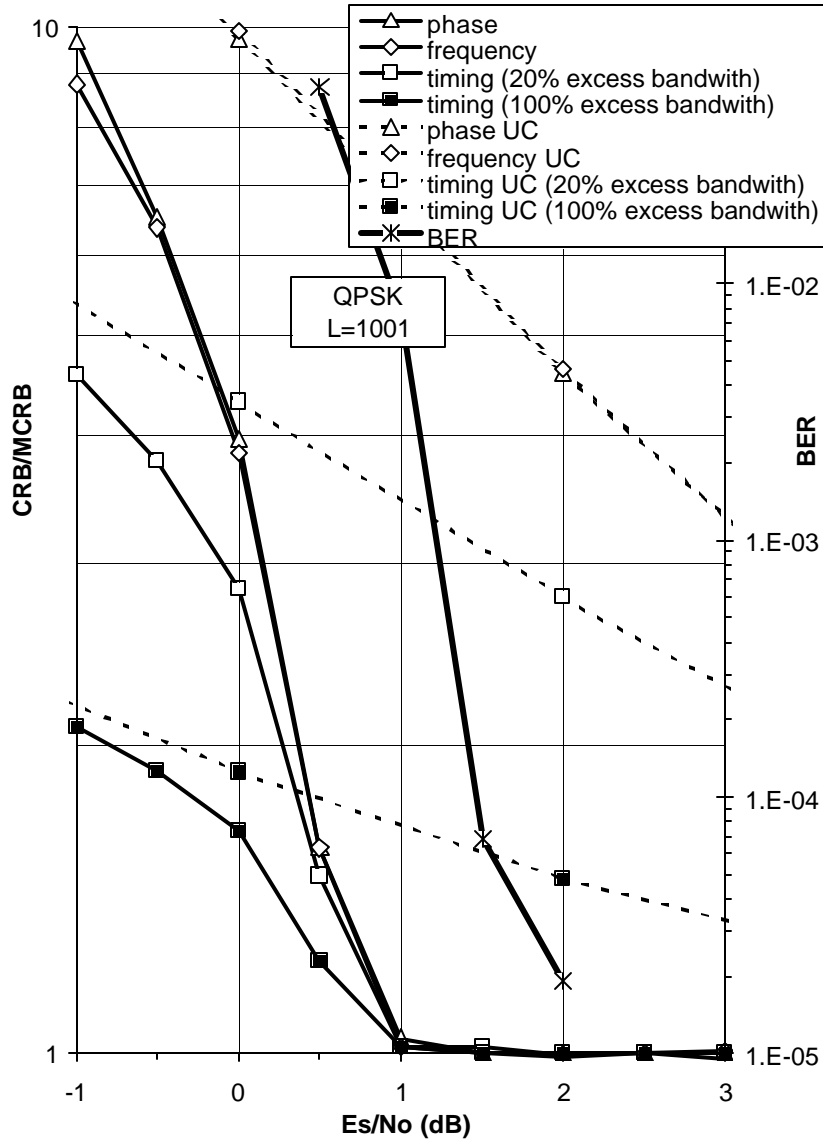


Fig.1: Comparison of the ratio CRB/MCRB for turbo encoded transmission with the ratio CRB/MCRB for uncoded (UC) transmission; for QPSK symbols and an observation length $L=1001$

V. ACTUAL ESTIMATOR PERFORMANCE

In this section we will show that CRB_{coded} and CRB_{uncoded} are useful benchmarks for the MSE resulting from code-ware and code-unaware synchronizers, respectively. Therefore we consider practical joint phase and frequency estimators, operating on the rate $\frac{1}{2}$ turbo-encoded QPSK signal from the previous section. We assume that the frequency offset does not exceed 10% of the baud rate, i.e., $|FT| \leq 0.1$. The MSE for phase and frequency estimation are shown as a function of the SNR in Figs. 2 and 3. As the joint estimation of carrier phase and frequency is only marginally affected by a small timing estimation error (because (θ, F) and τ are essentially decoupled), we have determined the mean square phase and frequency error assuming the timing to be known. An observation of $L=1001$ (i.e., block size of the code) unknown data symbols was considered. A preamble of N known pilot symbols (PS) at the beginning of each block may be used for initialization (to be explained in subsections V.A and V.B). A minimum of 10000

trials has been run; at each trial a new phase offset θ and a new frequency offset FT are taken from a uniform distribution over $[-\pi, \pi]$ and $[-0.1, 0.1]$, respectively.

Two algorithms for joint carrier phase and frequency estimation are considered.

- The conventional 4th-power Non Data Aided (NDA) synchronizer [14,15] is a code-unaware algorithm for carrier phase and frequency estimation that is very easy to implement. Moreover, this estimator was proposed in [16] for operation on a turbo-coded signal at very low E_s/N_0 . In contrast with the MSE of the code-aware estimators, the MSE of code-unaware estimators is lower bounded by the CRB_{uncoded} (with $CRB_{\text{uncoded}} \geq CRB_{\text{coded}}$). We will show that the MSE of this NDA synchronizer is close to CRB_{uncoded} , which indicates that this synchronizer is among the best code-unaware estimators.
- The soft Decision Directed (sDD) synchronizer from [8] is a code-aware algorithm that accepts soft information from the turbo decoder (i.e., 'turbo synchronization'). As motivated in [8], it involves a practical implementation of the maximum likelihood (ML) estimator by means of the expectation-maximization (EM) algorithm. This iterative algorithm converges to the ML estimate provided that the initial estimate is sufficiently accurate [17]. The ML estimator is known to become asymptotically unbiased and efficient (i.e., the MSE converges to CRB_{coded}) for an increasing number of observations. Therefore, we expect that the MSE performance of the sDD synchronizer from [8] will closely approach CRB_{coded} .

The phase error of the turbo synchronizer is measured modulo 2π and supported in the interval $[-\pi, \pi]$. The phase error of the NDA estimator was measured modulo $\pi/2$, i.e., in the interval $[-\pi/4, \pi/4]$, as the NDA estimator for QPSK gives a 4-fold phase ambiguity.

V.A Conventional (code-unaware) NDA estimator

The dashed curve in Figs. 2 and 3 corresponds to the MSE for carrier phase and frequency estimation, respectively, as obtained with the (code-unaware) conventional NDA estimator. For $E_s/N_0 \geq 3.5$ dB, the algorithm achieves near optimal CRB_{uncoded} performance. However, for $E_s/N_0 < 3.5$ dB, the performance of the frequency estimator dramatically deteriorates across a narrow SNR interval. This is the so-called *threshold phenomenon*, which is caused by the occurrence of large, spurious frequency errors (outliers) when the SNR drops below a certain threshold, and results in a very high frequency error variance at SNR below threshold [14], which also affects the accuracy of the phase estimate.

To show that the CRB_{uncoded} can be closely approached by the MSE resulting from code-unaware synchronizers even at low SNR, we replace the conventional NDA frequency estimation with the combined DA and NDA frequency estimation proposed in [18]. This approach consists of a two stage coarse-fine search. The DA estimator is used to coarsely locate the frequency offset, and then the more accurate NDA estimator attempts to improve the estimate within the residual uncertainty of the coarse estimator. In fact, the search range of the NDA estimator is restricted to the neighborhood of the peak of the DA-based likelihood function. This considerably reduces the probability to estimate an outlier frequency. As a result, the accuracy below threshold increases dramatically and the MSE approaches the CRB_{uncoded} . Moreover, the PS can be exploited to resolve the phase ambiguity: after frequency and phase correction, the samples of the preamble are compared to the known pilot symbols and, if necessary, an extra multiple of $\pi/2$ is compensated for.

In Figs. 2 and 3, the square markers illustrate the MSE for carrier phase and frequency estimation as obtained with this DA-NDA estimator, assuming the initial DA estimate is based on the observation of N preamble symbols. Results are displayed for $N=128$ and $N=256$. A threshold is still evident, but the performance below the SNR threshold degrades less rapidly than with the conventional NDA frequency estimator. The more PS are used, the more the threshold softens. Relatively large preambles are required for the DA-NDA estimator to perform closely to the $\text{CRB}_{\text{uncoded}}$, e.g. with $N=256$ the overhead $N/(N+L)$ equals about 20%.

Note that the SNR threshold can also be decreased by increasing the observation length (in [16], $L=8192$). However, enlarging the observation interval is not always possible. For the sake of completeness, we mention also that a more sophisticated distribution of the PS across the burst may reduce the number of PS required to obtain a certain DA estimation accuracy, thereby increasing the spectral efficiency of the transmission systems [18,19].

V.B Soft-decision-directed (code-aware) synchronizer

Let us consider the (code-aware) sDD synchronizer from [8] and compare its MSE to the new CRB for coded transmission. In our simulations, we used the approximate implementation proposed in [8]: at every turbo decoder iteration, soft decisions on the data symbols are extracted from the decoder and used to update the carrier phase and frequency estimates. This iterative sDD procedure was initialized with a Data Aided (DA) frequency and phase estimate obtained from the preamble, or with a combined DA-NDA frequency and phase estimate as described in subsection VI.A. We will refer to these synchronization schemes as DA-sDD and the DA-NDA-sDD, respectively. The PS are strictly used for the DA initialization, and the (NDA)-sDD algorithm uses only the L coded symbols; therefore, the $\text{CRB}_{\text{coded}}$ related to L symbols from section III is the appropriate lower bound on the performance of the sDD algorithms.

Our results indicate the importance of an accurate initial estimate. The curves marked with triangles (circles) in Figs. 2 and 3 show the MSE for carrier phase and frequency, respectively, as obtained with the DA-sDD (DA-NDA-sDD) estimator after 10 iterations of the turbo decoder/estimator. With $N=512$, the DA-sDD estimator performs very closely to the CRB. However, the resulting overhead of about 34% is often not acceptable. Reducing the number of PS to $N=256$ causes a serious degradation of the DA-sDD estimator. For a given number of PS, the DA-NDA-sDD estimator provides a considerable improvement over the DA-sDD estimator within the useful SNR range of the turbo code, and coincides with $\text{CRB}_{\text{coded}}$ at values of SNR larger than about 1.5 dB for $N=256$ (about 20% overhead) and 2 dB for $N=128$ (about 11% overhead).

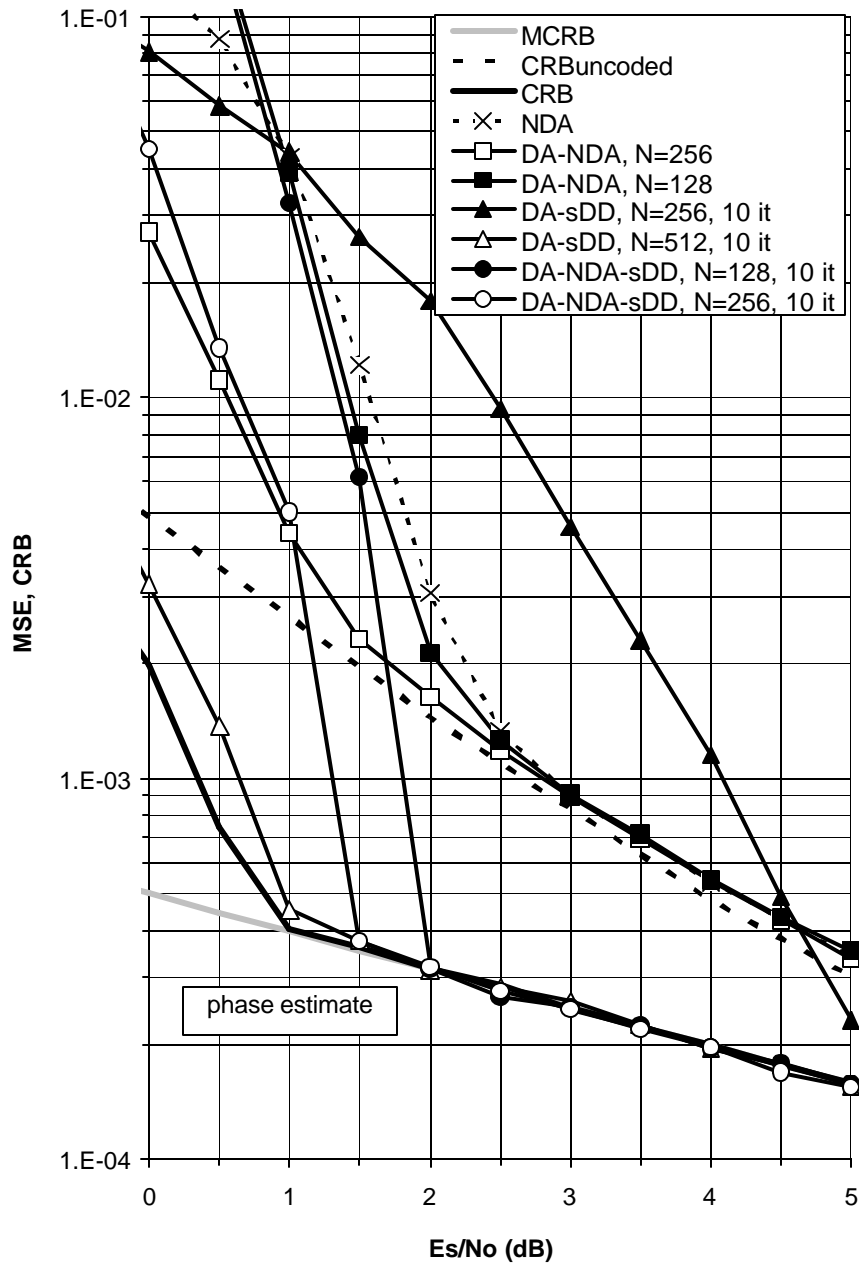


Fig.2: Comparison of the MSE of practical estimators with the CRB (phase estimate)

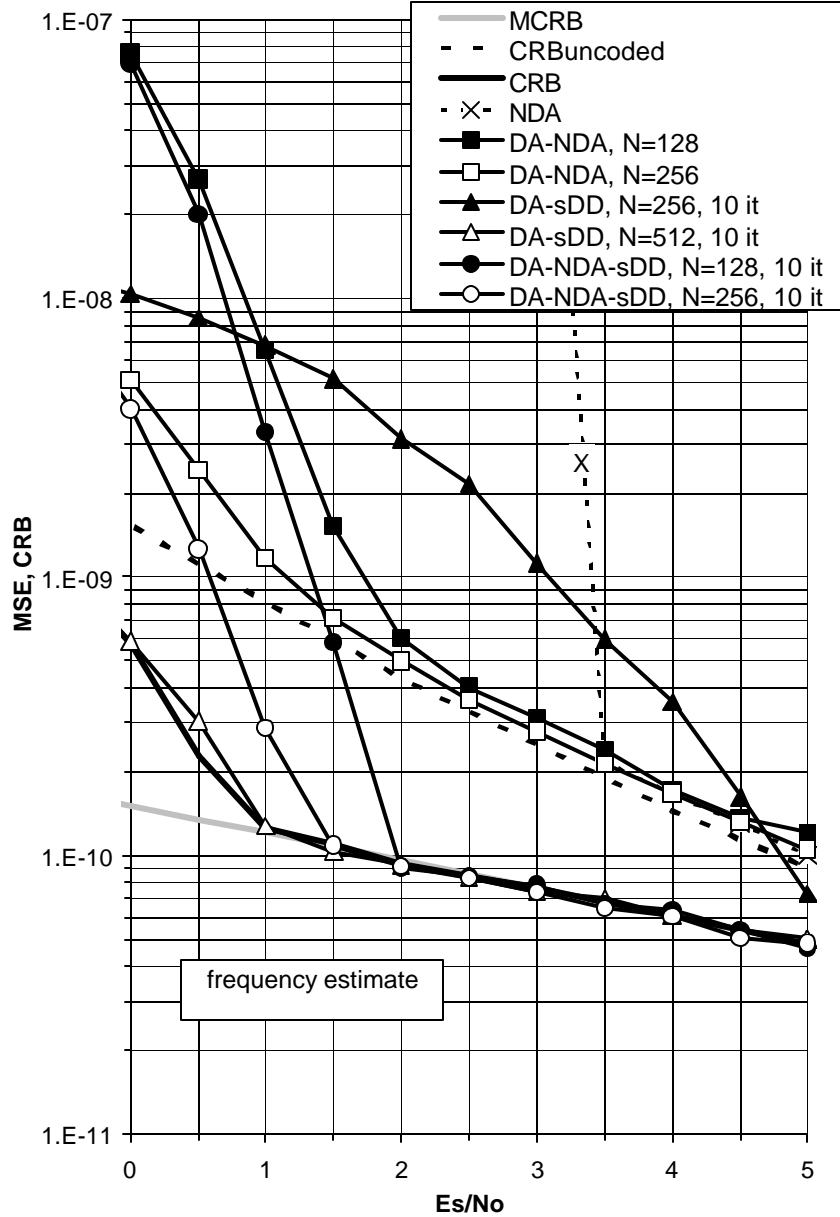


Fig.3: Comparison of the MSE of practical estimators with the CRB (frequency estimate)

VI. CONCLUSION

This contribution derives the CRB for joint carrier phase, carrier frequency offset and timing estimation from coded signals. The closed-form expression of the CRB in terms of the marginal symbol APPs allows efficient numerical evaluation. It was shown that, at the normal operating SNR of the code (say, $10^{-6} < \text{BER} < 10^{-3}$), the CRB is very close to the MCRB, which in turn is much less than the CRB for uncoded transmission. Furthermore, the CRB for uncoded transmission has been shown to lower bound the MSE of 'code-unaware' synchronizers that make no use of the code structure when operating on coded signals. This implies that in order to approach optimal performance, estimators should make clever use of the code

properties during the estimation process. The iterative code-aware turbo synchronizer for carrier phase and frequency estimation, presented in [8], has been shown to operate very closely to the CRB for coded transmission, provided that a sufficiently accurate initial estimate is available.

Although using a code-aware synchronizer instead of a code-unaware synchronizer substantially reduces the MSE at the normal operating SNR of the code, it highly depends on the specific coded system considered whether or not this reduction in MSE yields a considerable improvement in BER performance. In [16], code-unaware algorithms for carrier phase, carrier frequency and timing estimation that operate on a turbo-coded QPSK signal give rise to a BER degradation of only 0.05 dB as compared to a perfectly synchronized system: in this case, there is no need to use code-aware synchronization to further reduce the already very small BER degradation. On the other hand, [20] considers a different turbo-coded QPSK system, where the code-unaware 4th-power NDA phase synchronizer yields a BER degradation of about 1 dB at a BER of 10^{-3} , whereas code-aware phase synchronization reduces this BER degradation to about 0.05 dB only.

No performance results for practical timing estimators have been presented here. However, it has been shown in [21] that applying the turbo synchronization approach to timing estimation from coded signals results in a very low MSEE, which approaches the new CRB for timing estimation from section III.

VII. APPENDIX

For further use, we introduce the functions $g(t)$ and $f(t)$ given by :

$$g(t) = \int_{-\infty}^{+\infty} h(v)h(t+v)dv, \quad (\text{A.1})$$

$$f(t) = \int u^2 h(u)h(t+u)du \quad (\text{A.2})$$

and denote the first and second derivate of $g(t)$ with respect to t as $\dot{g}(t)$ and $\ddot{g}(t)$, respectively. Note that $g(t)$ is a Nyquist pulse: $g(kT) = \delta_k$. The pulses $g(t)$ and $\ddot{g}(t)$ are even in t , whereas $\dot{g}(t)$ is an odd function of t . For even $h(t)$, the function $f(t)$ is also even in t .

It follows from (17) that \mathbf{J}_{ij} can be expressed in terms of the following expectations :

$$\begin{aligned} E[\mathbf{m}_k^*(\tilde{\mathbf{z}})\mathbf{m}_k^*(\tilde{\mathbf{z}})\tilde{z}_{i,k}\tilde{z}_{j,k'}] &= E_{\tilde{\mathbf{z}}}[\mathbf{m}_k^*(\tilde{\mathbf{z}})\mathbf{m}_k^*(\tilde{\mathbf{z}})E[\tilde{z}_{i,k}\tilde{z}_{j,k'}|\tilde{\mathbf{z}}]], \\ E[\mathbf{m}_k^*(\tilde{\mathbf{z}})\mathbf{m}_k(\tilde{\mathbf{z}})\tilde{z}_{i,k}\tilde{z}_{j,k'}^*] &= E_{\tilde{\mathbf{z}}}[\mathbf{m}_k^*(\tilde{\mathbf{z}})\mathbf{m}_k(\tilde{\mathbf{z}})E[\tilde{z}_{i,k}\tilde{z}_{j,k'}^*|\tilde{\mathbf{z}}]], \end{aligned}$$

where $E_{\tilde{\mathbf{z}}}[\cdot]$ denotes averaging with respect to $\tilde{\mathbf{z}}$. The conditional expectations $E[\tilde{z}_{i,k}\tilde{z}_{j,k'}|\tilde{\mathbf{z}}]$ and $E[\tilde{z}_{i,k}\tilde{z}_{j,k'}^*|\tilde{\mathbf{z}}]$ can be determined analytically. One obtains

$$E[\tilde{z}_{q,k}\tilde{z}_{q,k'}|\tilde{\mathbf{z}}] = -\tilde{z}_k\tilde{z}_{k'}, \quad (\text{A.3})$$

$$E[\tilde{z}_{q,k}\tilde{z}_{q,k'}^*|\tilde{\mathbf{z}}] = \tilde{z}_k\tilde{z}_{k'}, \quad (\text{A.4})$$

$$E[\tilde{z}_{q,k}\tilde{z}_{F,k'}|\tilde{\mathbf{z}}] = 2\mathbf{p}(k'T + \mathbf{t})\tilde{z}_k\tilde{z}_{k'}, \quad (\text{A.5})$$

$$E[\tilde{z}_{q,k}\tilde{z}_{F,k'}^*|\tilde{\mathbf{z}}] = 2\mathbf{p}(k'T + \mathbf{t})\tilde{z}_k\tilde{z}_{k'}^*, \quad (\text{A.6})$$

$$E[\tilde{z}_{q,k}\tilde{z}_{t,k'}|\tilde{\mathbf{z}}] = -j\tilde{z}_k \sum_{m=-K}^K \tilde{z}_m \dot{g}(k'T - mT), \quad (\text{A.7})$$

$$E[\tilde{z}_{q,k} \tilde{z}_{t,k}^* | \tilde{\mathbf{z}}] = -j\tilde{z}_k \sum_{m=-K}^K \tilde{z}_m^* \dot{g}(k'T - mT), \quad (\text{A.8})$$

$$E[\tilde{z}_{F,k} \tilde{z}_{F,k'} | \tilde{\mathbf{z}}] = -4\mathbf{p}^2 \tilde{z}_k \tilde{z}_{k'} (kT + \mathbf{t})(k'T + \mathbf{t}), \quad (\text{A.9})$$

$$E[\tilde{z}_{F,k} \tilde{z}_{F,k'}^* | \tilde{\mathbf{z}}] = 4\mathbf{p}^2 \tilde{z}_k \tilde{z}_{k'}^* (kT + \mathbf{t})(k'T + \mathbf{t}) + 4\mathbf{p}^2 \frac{N_0}{E_s} f(kT - k'T), \quad (\text{A.10})$$

$$E[\tilde{z}_{F,k} \tilde{z}_{t,k'} | \tilde{\mathbf{z}}] = -j2\mathbf{p}(kT + \mathbf{t}) \tilde{z}_k \sum_{m=-K}^K \tilde{z}_m \dot{g}(k'T - mT), \quad (\text{A.11})$$

$$E[\tilde{z}_{F,k} \tilde{z}_{t,k'}^* | \tilde{\mathbf{z}}] = -j2\mathbf{p}(kT + \mathbf{t}) \tilde{z}_k \sum_{m=-K}^K \tilde{z}_m^* \dot{g}(k'T - mT) + j2\mathbf{p} \frac{N_0}{E_s} \left\{ -\frac{(kT - k'T)}{2} \dot{g}(kT - k'T) - \frac{1}{2} \mathbf{d}_{k-k'} \right\}, \quad (\text{A.12})$$

$$E[\tilde{z}_{t,k} \tilde{z}_{t,k'} | \tilde{\mathbf{z}}] = \sum_{m,n=-K}^K \tilde{z}_m \tilde{z}_n \dot{g}(kT - mT) \dot{g}(k'T - nT), \quad (\text{A.13})$$

$$E[\tilde{z}_{t,k} \tilde{z}_{t,k'}^* | \tilde{\mathbf{z}}] = \sum_{m,n=-K}^K \tilde{z}_m \tilde{z}_n^* \dot{g}(kT - mT) \dot{g}(k'T - nT) + \frac{N_0}{E_s} (-\ddot{g}(kT - k'T)) - \frac{N_0}{E_s} \sum_{m=-K}^K \dot{g}(kT - mT) \dot{g}(k'T - mT) \quad (\text{A.14})$$

Making use of (A.3)-(A.14), the evaluation of the FIM now requires *numerical* averaging over $\tilde{\mathbf{z}}$ only. This reduces the numerical complexity considerably.

Note from (A.5), (A.6), (A.9)-(A.12) that $\mathbf{J}_{\theta,F}$, $\mathbf{J}_{F,F}$ and $\mathbf{J}_{F,\tau}$ are a function of the parameter τ . This implies that the CRB depends on the exact value of the unknown but deterministic time delay $\tau \in [-T/2, T/2]$ that is being estimated. However, under the usual assumption that the observation interval is much longer than the symbol duration ($L \gg 1$), this dependence can be safely ignored, because we can use in (A.5), (A.6), (A.9)-(A.12) the approximations $kT + \tau \cong kT$ and $k'T + \tau \cong k'T$ when summing over k and k' in (17). A similar reasoning was made in [3] regarding the computation of the MCRB. Numerical results for different values of τ (not reported here) confirm this behavior.

VIII. REFERENCES

- [1] L.R. Bahl, J. Cocke, F. Jelinek and J. Raviv, "Optimal decoding of linear codes for minimizing symbol error rate," *IEEE Trans. Inform. Theory*, vol IT-20, pp. 248-287, March 1974.
- [2] A.N. D'Andrea, U. Mengali and R. Reggiannini, "The modified Cramer-Rao bound and its applications to synchronization problems," *IEEE Trans. Comm.*, vol COM-24, pp. 1391-1399, Feb.,Mar.,Apr. 1994.
- [3] F. Gini, R. Reggiannini and U. Mengali, "The modified Cramer-Rao bound in vector parameter estimation," *IEEE Trans. Commun.*, vol. CON-46, pp. 52-60, Jan. 1998
- [4] W.G. Cowley, "Phase and Fequency estimation for PSK packets: bounds and algorithms," *IEEE Trans. Comm.*, vol COM-44, pp. 26-28, Jan. 1996.

- [5] F. Rice, B. Cowley, B. Moran, M. Rice, "Cramer-Rao lower bounds for QAM phase and frequency estimation," *IEEE Trans. Commun.*, vol. 49, pp 1582-1591, Sep. 2001
- [6] N. Noels, H. Steendam and M. Moeneclaey, "The true Cramer-Rao Bound for Carrier Frequency Estimation from a PSK signal", accepted for publication in *IEEE Trans. Commun.*, 2004
- [7] N. Noels, H. Steendam and M. Moeneclaey, "The true Cramer-Rao bound for timing recovery from a bandlimited linearly modulated waveform with unknown carrier phase and frequency," *IEEE Trans. Commun.*, vol. 52, No. 3, pp. 473-483, March 2004
- [8] N. Noels et Al., "Turbo Synchronization: an EM algorithm interpretation," in *Proc. IEEE Int. Conf. Comm. 2003*, Anchorage, Alaska, Paper CT22-2, May 2003.
- [9] H.L. Van Trees, *Detection, Estimation and Modulation Theory*, New York: Wiley, 1968
- [10] N. Noels, H. Steendam, M. Moeneclaey, "The Cramer-Rao Bound for Phase Estimation from Coded Linearly Modulated Signals," *IEEE Communication Letters*, vol. 7, No. 5, pp. 207-209, May 2003
- [11] M. Moeneclaey, "On the true and modified Cramer-Rao bounds for the estimation of a scalar parameter in the presence of nuisance parameters," *IEEE Trans. Comm.*, vol COM-46, pp. 1536-1544, Nov. 1998.
- [12] C. Berrou and A. Glavieux, "Near Optimum Error correcting Coding and Decoding: Turbo codes," *IEEE Trans. Commun.*, vol. 44, pp 1261-1271, Oct. 1996
- [13] T. Richardson, "The geometry of turbo-decoding dynamics," *IEEE Trans. Inf. Theory*, vol. 46, pp 9-23, Jan 2000
- [14] D.C. Rife and R.R. Boorstyn, "Single tone parameter estimation from discrete-time observations," *IEEE Trans. Inform. Theory*, vol. IT-20, pp. 591-598, Sept. 1974
- [15] A.J. Viterbi and A.M. Viterbi, "Nonlinear estimation of PSK-modulated carrier phase with application to burst digital transmission," *IEEE Trans. Inform. Theory*, vol. IT-29, pp. 543-551, July 1983
- [16] A. D'Amico, A.N. D'Andrea and R. Reggiannini, "Efficient Non-Data-Aided Carrier and Clock Recovery for Satellite DVB at Very Low Signal-to-Noise Ratios," *IEEE Journal on selected areas in communications*, vol. 19, No. 12, pp. 2320-2330, Dec. 2001
- [17] R.A. Boyles, "On the convergence of the EM algorithm," *J.R.Statist. Soc. B*, 45, No. 1, pp.47-50, 1983
- [18] B. Beahan and B. Cowley, "Frequency Estimation of Partitioned Reference Symbol Sequences," master thesis supervisor B. Cowley, www.itr.unisa.edu.au/~steven/thesis
- [19] J.A. Gansman, J.V. Krogmeier and M.P. Fitz, "Single Frequency Estimation with Non-Uniform Sampling," in *Proc. of the 13th Asilomar Conference on Signals, Systems and Computers*, Pacific Grove, CA, pp.878-882, Nov. 1996
- [20] H. Wymeersch, N. Noels, H. Steendam and M. Moeneclaey, "Synchronization at low SNR : performance bounds and algorithms," presented at *IEEE Communication Theory Workshop*, Capri, Italy, May 5-8, 2004
- [21] C. Herzet, V. Ramon, L.Vandendorpe and M. Moeneclaey, "EM algorithm-based timing synchronization in turbo receivers," in *Proc. ICASSP 2003*, Hong Kong, April 2003